Hindawi
Advances in Condensed Matter Physics
Volume 2019, Article ID 4715953, 8 pages
https://doi.org/10.1155/2019/4715953

Research Article

Electronic Transport in the V-Shaped Edge Distorted Zigzag Graphene Nanoribbons with Substitutional Doping

Nguyen Thanh Tien,[1] **Nguyen Van Ut**,[1] **Bui Thai Hoc**,[1] **Tran Thi Ngoc Thao**,[1] **and Nguyen Duy Khanh**[2]

[1]*College of Natural Science, Can Tho University, 3-2 Road, Can Tho City, Vietnam*
[2]*Department of Physics, National Cheng Kung University, Tainan, Taiwan*

Correspondence should be addressed to Nguyen Thanh Tien; thanhtienctu@gmail.com

Received 17 June 2018; Revised 17 September 2018; Accepted 27 December 2018; Published 12 February 2019

Academic Editor: Jörg Fink

Density-functional theory (DFT) in combination with the nonequilibrium Green's function formalism is used to study the effect of substitutional doping on the electronic transport properties of V-shaped edge distorted zigzag graphene nanoribbons (DZGNRs), in which DZGNRs with the various widths of four-, six-, and eight-zigzag chains are passivated by H atoms. In this work, Si atoms are used to substitute carbon atoms located at the center of the samples. Our calculated results have determined that Si can change the material type by the number of dopants. We found that the transmission spectrum strongly depends on the various widths. The width of eight-zigzag chains exhibits the largest transmission among four- and six-zigzag chains, and the single Si substitution presents larger transmission than the double case. The obtained results are explained in terms of electron localization in the system due to the presence of distortion at edge and impurities. The relationships between the transmission spectrum, the device density of states, and the I-V curves indicate that DZGNRs are the highly potential material for electronic nanodevices.

1. Introduction

Graphene, a two-dimensional (2D) nanomaterial arising from a hexagonal carbon lattice in a single layer, has been widely regarded as the most promising candidate for the application of the next generation of nanodevices since its fabrication in 2004 by Novoselov and coworkers [1]. Many experimental developments, together with the fascinating physicochemical properties of graphene, have stimulated extensive experimental and theoretical studies [2, 3]. However, graphene is a gapless material. To induce an electronic band gap, the graphene sheets are patterned into ribbons, which are so called graphene nanoribbons (GNRs) [4]. The outstanding properties of GNRs are well known nowadays: their electronic properties strongly depend on the shape, width, length, and edge morphology [5, 6]. It has been recently demonstrated that all these variables can be fully engineered. Chemical doping is a powerful method to modify the electronic properties of carbon-based nanomaterials and, hence, it could be used to customize the electronic and quantum transport properties of GNRs [7].

Nano-sized graphene nanoribbons have been cut out of graphene sheets with two basic shapes for the edges: armchair and zigzag, which have distinct electronic transport properties [8]. The electronic transport properties of GNRs are sensitive to many factors, such as doping, defects, edge modification, molecule adsorption, and external electrical field [9–13]. The essential modifications provide many possibilities to adjust and significantly expand or anticipate difficulties in the application of GNRs. Besides, the GNRs in the real devices are imperfections. It can be deformed at the edge or tailored on the edge [10]. We can investigate the influence of structural distortion and chemical defects on transport properties of the zPNR devices. Such a study is very essential to design experimental structures. The edge-tailored GNRs are expected to exhibit the potential transport properties. Therefore, the exotic electronic transport properties in the edge distorted zigzag graphene nanoribbons deserve a systematic study.

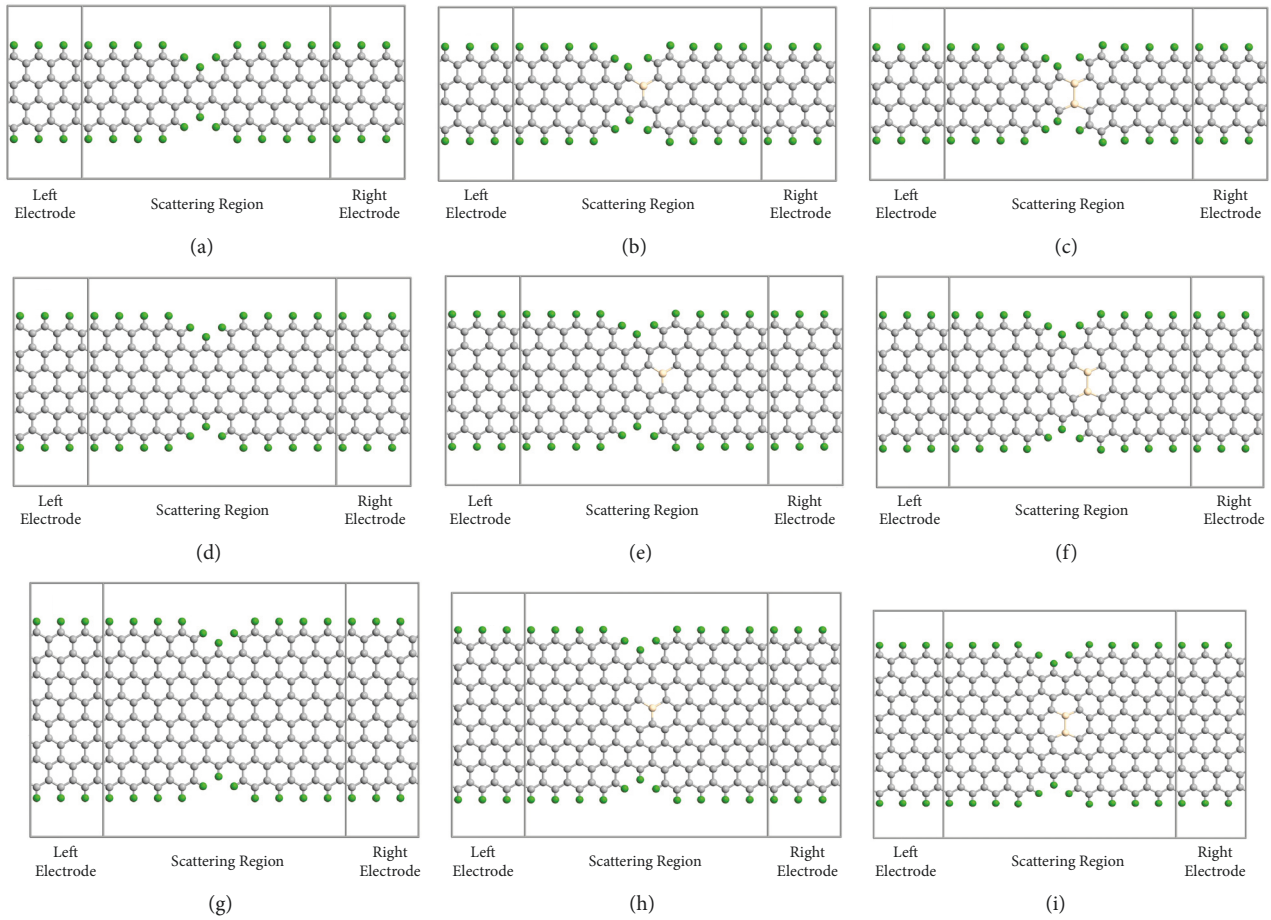

Figure 1: Schematic (top view and side view) of device geometries: (a) 4-DZGNR, (b) Si-4-DZGNR, (c) 2Si-4-DZGNR, (d) 6-DZGNR, (e) Si-6-DZGNR, (f) 2Si-6-DZGNR, (g) 8-DZGNR, (h) Si-8-DZGNR, and (i) 2Si-8-DZGNR. The hydrogen-passivated V-shaped edge DZGNRs with the single Si substitution ((b), (e), and (h)) and the double one ((c), (f), and (i)) at the center of the models.

In the present work, we explore in detail the electronic transport properties of the V-shaped edge distorted zigzag graphene nanoribbons with Si substitutional doping. The paper is organized as follows. In Section 2, the models and computational methods are discussed, and the formulas related to the transport properties are derived. Section 3 demonstrates the results and discussion concerning the effect of numbers of zigzag chains and the effect of numbers of dopant atoms on the electronic transport properties. We also illustrate the current–voltage (I–V) curves as a function of bias. Finally, Section 4 presents the conclusions.

2. Models and Method

We study the hydrogen-passivated distorted ZGNRs (DZGNRs) under the various widths with/without Si atoms substitution, as illustrated in Figure 1: (a) the distorted ZGNR with the width of four-zigzag chains (4-DZGNR), (b) the single Si atom-substituted 4-DZGNR (Si-4-DZGNR), (c) the double Si atoms-substituted 4-DZGNR (2Si-4-DZGNR), (d) the distorted ZGNR with the width of six-zigzag chains (6-DZGNR), (e) the single Si atom-substituted 6-DZGNR (Si-6-DZGNR), (f) the double Si atoms-substituted 6-DZGNR (2Si-6-DZGNR), (g) the distorted ZGNR with the width of eight-zigzag chains (8-DZGNR), (h) the single Si atom-substituted 8-DZGNR (Si-8-DZGNR), and (i) the double Si atoms-substituted 8-ZGNR (2Si-8-DZGNR). The left and right electrodes of each device are semi-infinite unit cells repeated along the z axis.

First-principles calculations based on density functional theory (DFT) and nonequilibrium Green's function (NEGF) formalism implemented in the Atomistix ToolKit (ATK) software package (version 2016.4) [14, 15] are used to investigate the electronic transport properties of distorted and doped zigzag graphene nanoribbons (ZGNRs) with H passivation. All considered samples are first optimized using DFT calculations within the generalized gradient approximation (GGA) of Perdew–Burke–Ernzerhof (PBE) for the exchange-correlation energy [16]. The Brillouin zone sampling is performed using 1 x 1 x 12 k-point sampling [17]. The electrostatic potentials are determined on a real-space grid with a mesh cutoff energy of 150 Ry. The electron wave function is expended using double-zeta-double-polarized basis set. Van der Waals interactions were accounted for by using

Grimme's DFT-D2 empirical dispersion correction [18] to the PBE. Using the optimized structures, we construct device geometries, which consist of three regions: left electrode, central scattering region, and right electrode. Each electrode consists of 3 unit cells with a length of 7.38 Å and the length of the scattering region in each device is 24.61 Å [19]. The electrodes are modeled as an electron gas with a fixed chemical potential. The transmission is calculated along the z-direction. The quantum transport properties are calculated by NEGF formalism within the Brilouin zone sample of 1x1x100 k-points meshes.

The current is calculated by integrating the transmission function over the energy bias window by the following formula [20]:

$$I(V_b) = \frac{2e}{h}\int_{-\infty}^{\infty} T(E, V_b)\left[f(E-\mu_L) - f(E-\mu_R)\right]dE, \quad (1)$$

where $T(E, V_b)$ is the transmission function at energy E and bias V_b using the Landauer formula [21]; $f(E-\mu_{L/R})$ are the Fermi distribution functions of the electrons in the electrodes with $\mu_L = E_f + eV_b/2$ and $\mu_R = E_f - eV_b/2$ being the electrochemical potentials of the left and right electrodes, in which E_F is the Fermi energy at zero bias.

3. Results and Discussion

To obtain stable geometry structures of the distorted and doped systems, we optimize the atomic structure of each DZGNR. Numerical results show that, after doping, Si atoms stay in the same plane of graphene, the lattice constants have slight changes and also local changes of the bond lengths and bond angles [22, 23] (Figure 1).

3.1. The Effect of the Various Widths on Transport Properties. The transmission spectra T(E) and device density of states (DDOS) at zero bias voltage provide much useful information to investigate the various widths effects on the electronic transport of the ZGNRs and the DZGNRs, as illustrated in Figure 2.

In the case of ZGNRs (Figure 2(a)), T(E) exhibits a sequence of steps of integer transmission (T(E) ~ 1 around Fermi level) and an enhanced transmission and the same for three samples at the Fermi level, which are characteristic features of zigzag graphene nanoribbons, whereas the samples exhibit broad around the Fermi level decreases when numbers zigzag chains increases from 4 [-2.28 eV, 1.74 eV] to 6 [-1.68 eV, 1.38 eV] and 8 [-1.32 eV, 1.14 eV] zigzag chains. These features derive from the edge-localized electronic states with energies close to the Fermi energy [22].

The transmission spectrum presents the dramatic change when the edge carbon atoms are distorted, as indicated in Figure 2(c). T(E) becomes smaller at the Fermi level and it slightly increases with increasing numbers of zigzag chains and broad around Fermi level decreases with ZGNRs samples, respectively. Exceptionally, the value of transmission spectrum T(E) at the Fermi level of 4-DZGNR shows lager transmission as compared to the other two samples and it drops sharply with decreasing electron energy away from the Fermi energy [-2.82 eV]. In fact, electrons can be totally reflected at these small energies. Interestingly, the obtained valleys in the transmission curves are reflected in the DDOS as peaks at the same electron energies in the range of [-2.5 eV, 2.5 eV] (see short-doted-blue curves in Figure 2(d)). In particularly, T(E) of 6-DZGNR and 8-DZGNR vary greatly in the energy range far from the Fermi level compared to the T(E) of 4-DZGNR. This leads to significant changes in the I-V curves discussed in the next section.

Figures 3(a) and 3(b) shows the obtained results in regard to T(E) and DDOS for the samples with substitutional doping at center. The transmission of a single Si doped samples increases slightly with increasing number zigzag chains. Meanwhile, the value of T(E) of Si-4-DZGNR is largest at Fermi level (Figure 3(a)). Next, we consider the case of double carbon substitutions but only dimer impurities are considered. Impurities are put at adjacent sites and hence we do not aim to probe impurity-impurity correlation effects [24]. As main results, we show in Figures 3(c) and 3(d) the zero voltage transmission spectra and the device density of states. In case of zero voltage, the results are similar to Si-DZGNR samples. The transmission spectrum changes drastically in case the distorted graphene nanoribbons with two Si atoms appearance at the middle. T(E) becomes smaller at the Fermi level and it slightly increases with increasing zigzag chain number and broadening around Fermi level decreases. Exceptionally, the value T(E) of 2Si-4-DZGNR is largest. Meanwhile, the T(E) of 6-2Si-DZGNR is larger than one of 2Si-8-DZGNR samples at the Fermi level (Figure 3(c)). Profound minima in the transmission spectrum are also obtained for the 2Si-4-DZGNR sample, which also originates from the strong localization of the electronic states in the system.

3.2. The Effect of Numbers of Dopant Atoms on the Transport Properties. To compare and evaluate the effect of numbers of dopant atoms on T(E), we redraw the transmission spectra and device density of states at zero voltage in Figure 4. Solid-black curves show the results for pristine ZGNR as a reference. The ZGNR samples have a good symmetry and a great transmittance near the Fermi surface. As the Si atoms substitute the middle carbon atoms, they introduce impurities [25]. The scattering of electrons and impurity atoms are enhanced in the systems. The scattering of impurities rises as the number of Si dopants increases so the transmittance of electrons near the Fermi level becomes small. T(E) becomes smaller at the Fermi level and it drops sharply with increasing (or decreasing) electron energy away from the Fermi energy. It can be seen obviously that, in Si-4-DZGNR and 2Si-4-DZGNR, the transmission coefficient at -2.82 eV energy is near zero, which indicates that scattering is greater than that in the ZGNR sample. Interestingly, there is a strong relationship between T(E) and DDOS. The ZGNR samples have a high density of electronic states at the Fermi level, which exhibits metallic behavior. Nevertheless, the Fermi peak decreases considerably due to the number of Si atoms and a new peak appears after Si-doping. These obtained peaks far away Fermi level are reflected as minima in the same electron energies in T(E).

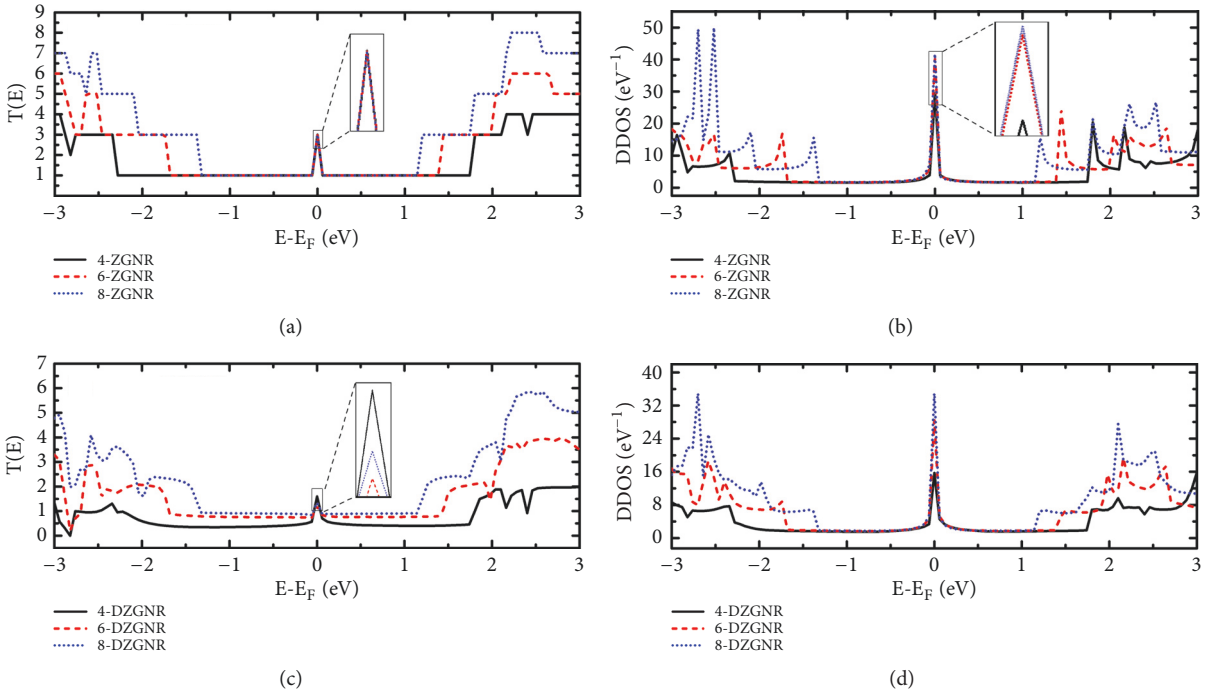

FIGURE 2: Transmission spectrum, T(E) ((a), (c)) and the device density of states, DDOS ((b), (d)) as a function of electron energy at zero bias voltage. The results are shown for a pristine graphene ribbon as a reference (a) and a distorted graphene ribbon (c) with four zigzag chains (solid-black curve) and for six zigzag chains (short-dashed-red curve) and for eight zigzag chains (short-dotted-blue curve) in width.

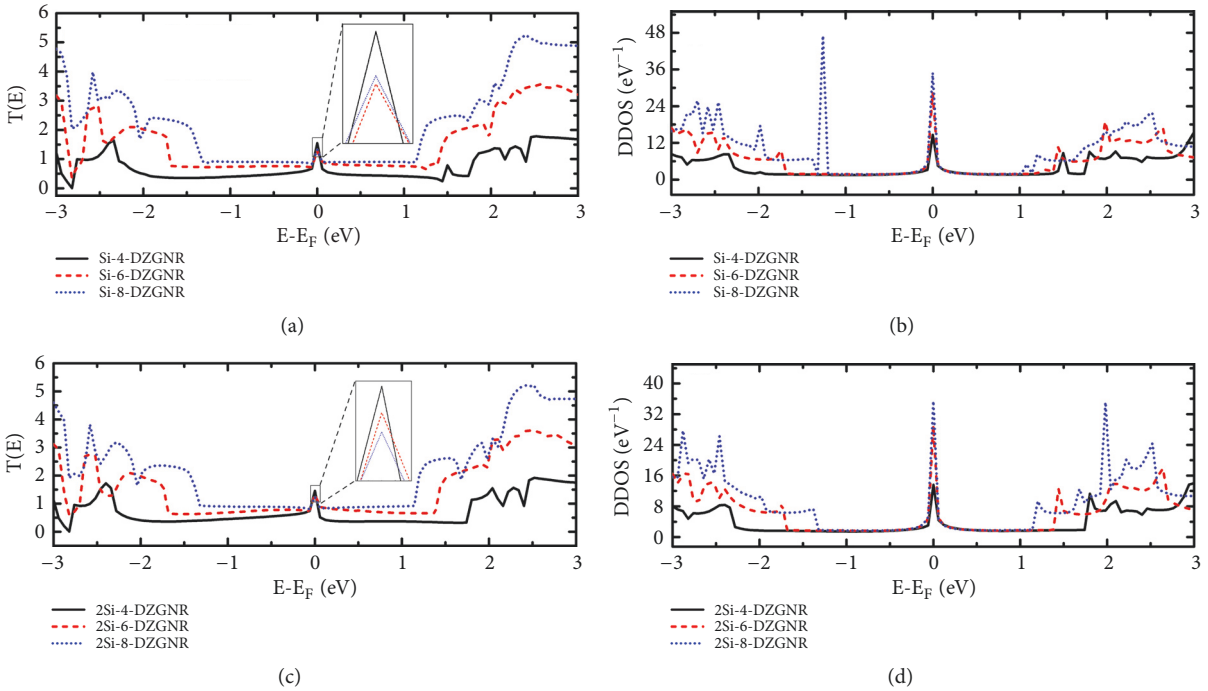

FIGURE 3: The same plot as Figure 2, the results are shown for distorted graphene with a single (a) and a double (c) middle substitution with Si atoms for four zigzag chains (solid-black curve) and for six zigzag chains (short-dashed-red curve) and for eight zigzag chains (short-dotted-blue curve) in width.

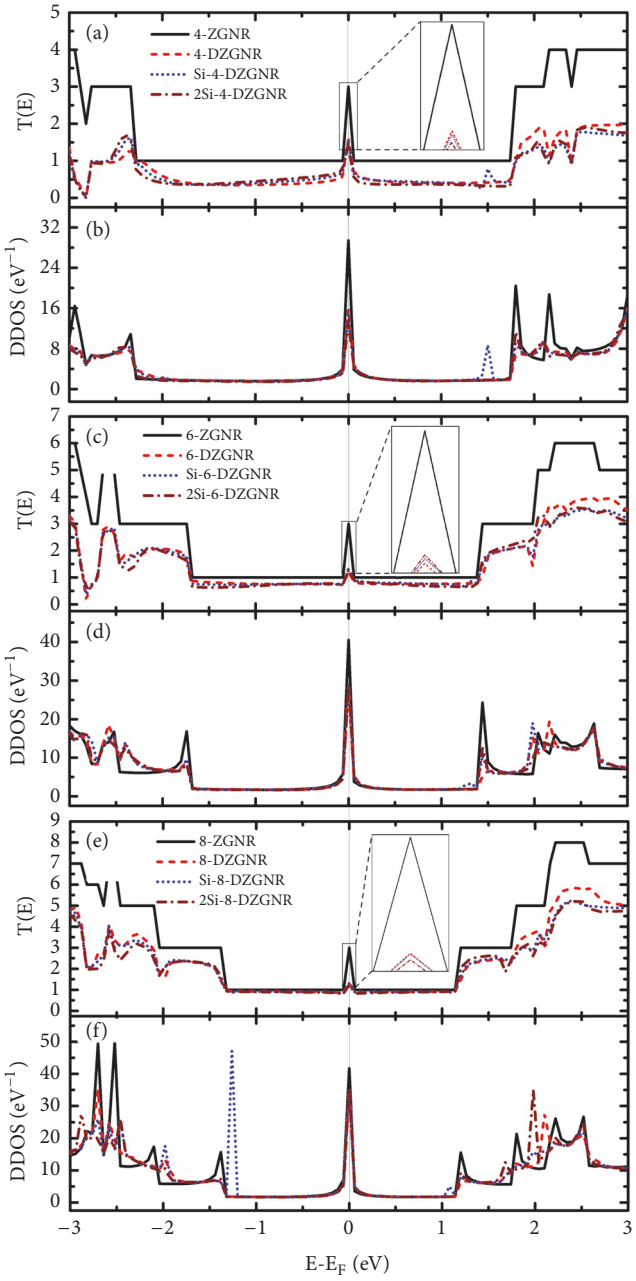

FIGURE 4: Transmission spectrum T(E)((a), (c), and (e)) and device density of states DDOS ((b), (d), and (f)) as a function of electron energy at zero bias voltage. The results are shown for four zigzag chains (a), six zigzag chains (c), and eight zigzag chains (e) the samples.

In order to analyze the contribution of the dopant atoms to the transport properties of the studied systems, Figure 5 describes the projected density of states (PDOS) of (Si-4-DZGNR, 2Si-4-DZGNR-Figures 5(a) and 5(b)), (Si-6-DZGNR, 2Si-6-DZGNR - Figures 5(c) and 5(d)), and (Si-8-DZGNR, 2Si-8-DZGNR-Figures 5(e) and 5(f)). In all cases, the contribution of s orbital is negligible; only the contribution of d orbital is appreciable. In the case of Si-4-DZGNR (Figure 5(a)), the largest contribution of dopant

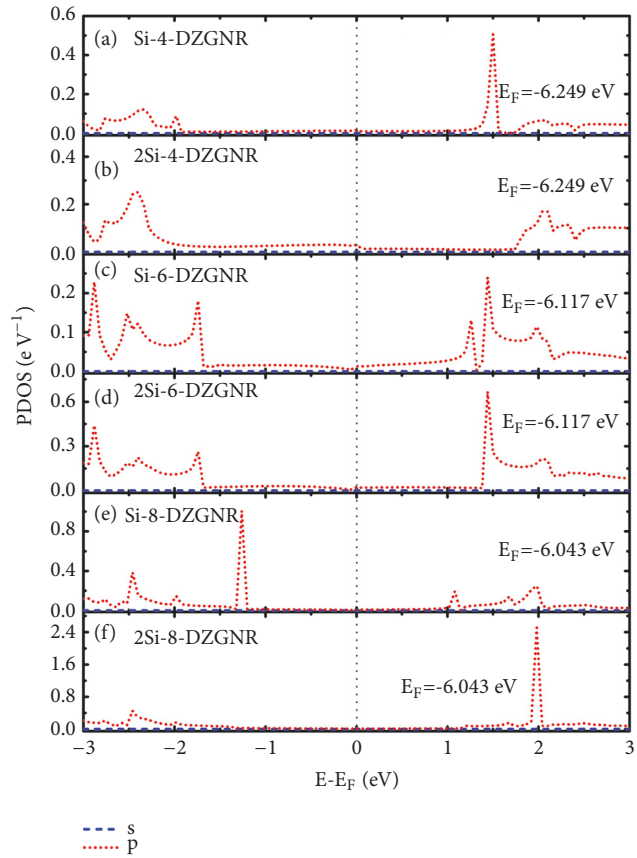

FIGURE 5: Partial density of states PDOS of Si in two structures: (a) Si-4-DZGNR and (b) 2Si-4-DZGNR.

atom is obtained at the energy 1.5 eV. This is also reflected in the device density of states (Figure 4(b)). The contribution of Si atom becomes less obvious far away from the Fermi level. In contrast, the dominant contribution of Si atom only appears away from Fermi level in 2Si-4-DZGNR, as shown in Figure 5(b). The peaks of PDOSs of the other cases ((Si-6-DZGNR, 2Si-6-DZGNR) and (Si-8-DZGNR, 2Si-8-DZGNR)) have varied and are also reflected in the device density of states (Figures 4(d) and 4(f)).

3.3. The Current–Voltage (I–V) Curves. To explore the anisotropic transport properties, in Figure 6, we further illustrate the current–voltage (I–V) curves.

The results show that the value of current increases with increasing number of zigzag chains and there is an obvious circulating in the voltage range from 0.2 V to 1.4 V for both samples ZGNR (Figure 6(a)) and DZGNR (Figure 6(b)), which indicates that the negative differential resistance (NDR) behavior occurs in the samples [26], whereas the 6-DZGNR and the 8-DZGNR sample increased sharply with a voltage range of 1.4 V to 2.0 V (b). Remarkably, at the 2.0 V voltage, the current of the 6-DZGNR (~6.0 μA) is twice as large as the current of the 4-DZGNR (~3.0 μA). Similarly, the current of the 8-DZGNR (~12.0 μA) is twice as large as the current of the 6-DZGNR.

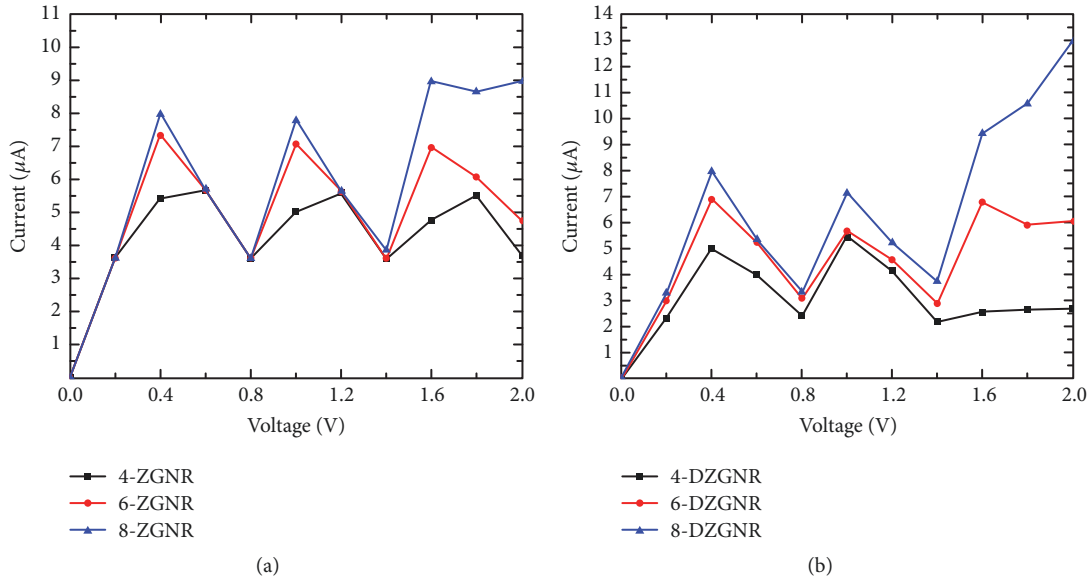

Figure 6: Calculated I-V curves for six structures: (a) 4-ZGNR, 6-ZGNR, and 8-ZGNR and (b) 4-DZGNR, 6-DZGNR, and 8-DZGNR.

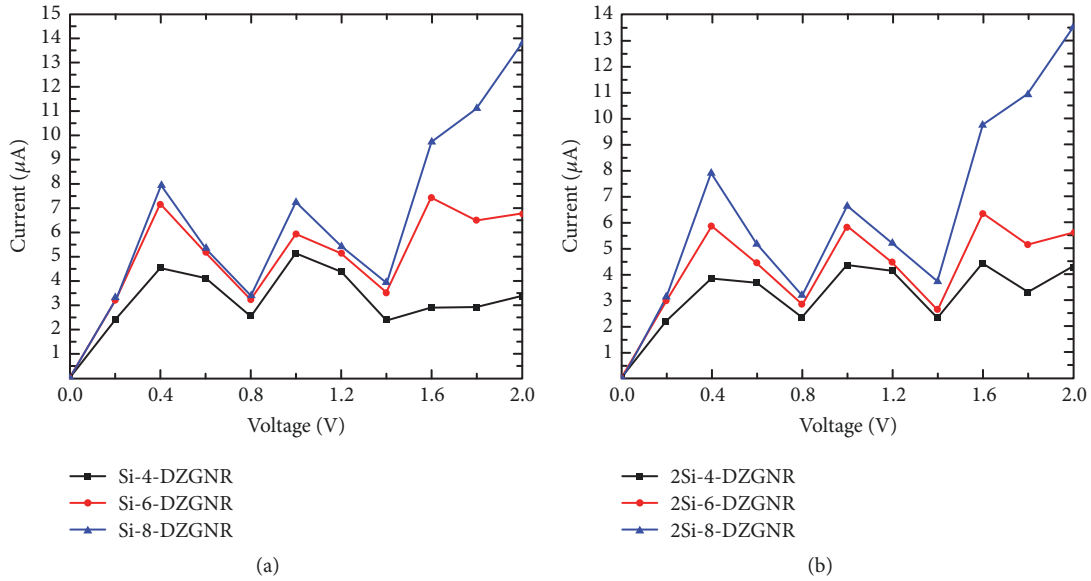

Figure 7: Calculated I-V curves for six structures: (a) Si-4-DZGNR, Si-6-DZGNR, and Si-8-DZGNR and (b) 2Si-4-DZGNR, 2Si-6-DZGNR, and 2Si-8-DZGNR.

Figure 7 shows the same result as Figure 6; the current increases linearly from 0.0 V to 0.2 V and increases sharply from 1.4 V to 2.0 V in the samples. In addition, we can see that when increasing the number of zigzag chains in samples, the current intensity in case of the eight zigzag chains is higher than the one of other samples. This is due to a significant reduced scattering at the boundary of the structure by the following: the smaller the size of V-shaped edges, the larger the structure of the samples.

In order to understand the $(I–V)$ curves of the DZGNR, we illustrate the transmission spectra of the 8-DZGNR at the different bias voltages as an example in Figure 8. It is evident that, at zero bias, there is a peak transmission at the Fermi level, so the value of the current is 0 A. As bias increases from zero to 2.0 V, the energy gap appears and becomes more widened in the samples, which contributes to the transformation from half-metallicity to semiconductor. Samples showing zero transmission coefficients are still observed for the values of the applied voltage near the Fermi level. However, as the applied voltage is 2.0 V, the area of the plane bounded by $T(E)$ curve and the horizontal axis from - 1.0 V to 1.0 V becomes significant. This explains why the current of sample 8-DZGNR is significant compared to other samples. Moreover, Figure 8 also shows that the integration area changes monotonically with bias, leading to the NDR behavior.

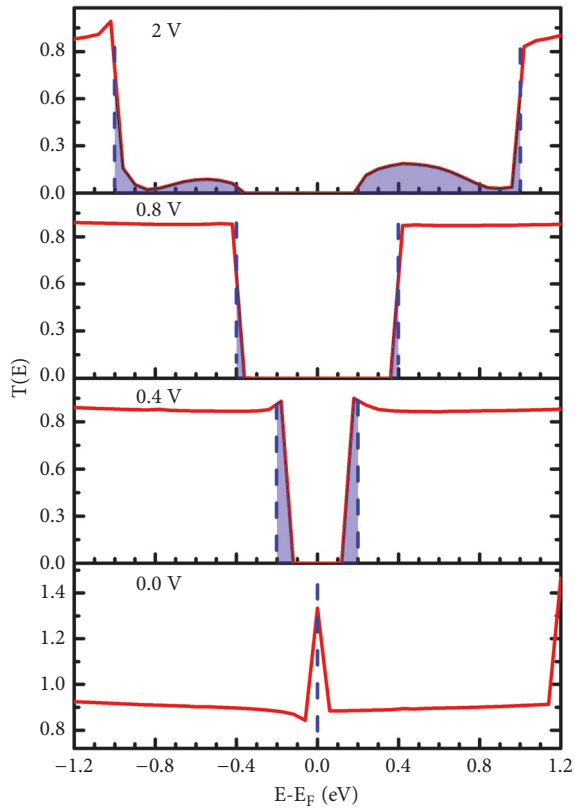

Figure 8: Transmission spectra of 8-DZGNR at different bias voltages (△V = 0.0 V, 0.4 V, 0.8 V, and 2.0 V). The vertical dashed lines represent the bias windows.

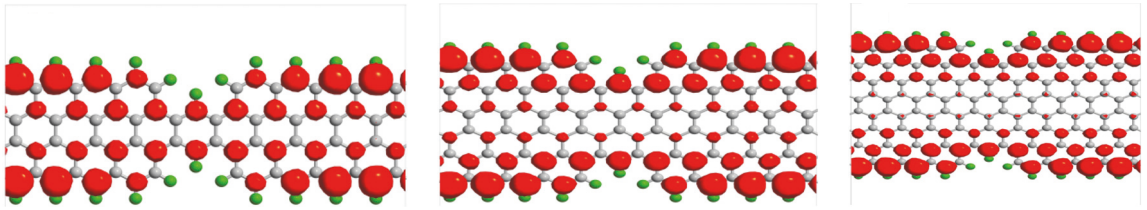

Figure 9: The isosurface of spatial electron distribution for the (a) 4-DZGNR, (b) 6-DZGNR, and (c) 8-DZGNR structures, respectively, at bias zero and Fermi energy point.

To illustrate more clearly the role of the edge-localized electronic state on the electronic transport properties, we plot the isosurface of spatial electron distribution for the DZGNR structures at bias zero and Fermi energy point in Figure 9. It is clear that the electron localization in the system is due to the presence of edge and the distortion at edge. This electron localization phenomenon governs the electronic transport strongly. We also determined that the electron localization due to the presence of impurities is less important.

4. Conclusion

In summary, we calculated the electronic transport properties of hydrogen passivated V-shaped edge distorted zigzag graphene nanoribbons using first-principles calculations based on nonequilibrium Green's function combined with the DFT method. The results indicate that

(i) the value of T(E) becomes smaller at the Fermi level and it slightly increases with increasing zigzag chain number: T(E) broad around Fermi level, a transformation from half-metallicity to semiconductor even if zero bias voltage.

(ii) the value of T(E) does not differ significantly when the Si dopants locate in the middle of device but the peak of T(E) at Fermi level decreases considerably and a new peak appear.

(iii) the value of current increases with increasing the number of zigzag chain and the NDR behavior is observed. Moreover, the (I–V) curves increased sharply with high voltage range.

We expect that this systematic study will be useful to further investigate experimentally the transport properties and related devices of studied samples [27].

Data Availability

No data were used to support this study.

Disclosure

This work was presented as poster at 43rd National Conference on Theoretical Physics (NCTP-43-Vietnam).

Conflicts of Interest

The authors declare that they have no conflicts of interest.

Acknowledgments

This research is funded by Vietnam National Foundation for Science and Technology Development (NAFOSTED) under Grant number 103.01-2017.74. Also, the authors would like to thank the Swedish National Infrastructure for Computing (SNIC) for the computational support.

References

[1] K. S. Novoselov, A. K. Geim, S. V. Morozov et al., "Two-dimensional gas of massless Dirac fermions in graphene," *Nature*, vol. 438, no. 7065, pp. 197–200, 2005.

[2] M. Y. Han, B. Özyilmaz, Y. Zhang, and P. Kim, "Energy band-gap engineering of graphene nanoribbons," *Physical Review Letters*, vol. 98, no. 20, Article ID 206805, 2007.

[3] P. Avouris and C. Dimitrakopoulos, "Graphene: synthesis and applications," *Materials Today*, vol. 15, no. 3, pp. 86–97, 2012.

[4] M. Y. Han, B. Özyilmaz, Y. Zhang, and P. Kim, "Energy band-gap engineering of graphene nanoribbons," *Physical Review Letters*, vol. 98, Article ID 206805, 2007.

[5] C. Wu, J. Chai, and J. Chem, "Electronic properties of zigzag graphene nanoribbons studied by TAO-DFT," *Journal of Chemical Theory and Computation*, vol. 11, no. 5, pp. 2003–2011, 2015.

[6] H. Teong, K. Lam, S. B. Khalid, and G. Liang, "Shape effects in graphene nanoribbon resonant tunneling diodes: A computational study," *Journal of Applied Physics*, vol. 105, no. 8, Article ID 084317, 2009.

[7] A. H. Castro Neto, F. Guinea, N. M. R. Peres, K. S. Novoselov, and A. K. Geim, "The electronic properties of graphene," *Reviews of Modern Physics*, vol. 81, no. 1, pp. 109–162, 2009.

[8] L. Brey and H. A. Fertig, "Electronic states of graphene nanoribbons studied with the Dirac equation," *Physical Review B: Condensed Matter and Materials Physics*, vol. 73, no. 23, Article ID 235411, 2006.

[9] B. Biel, X. Blase, F. Triozon, and S. Roche, "Anomalous doping effects on charge transport in graphene nanoribbons," *Physical Review Letters*, vol. 102, no. 9, Article ID 096803, 2009.

[10] F. Cervantes-Sodi, G. Csányi, S. Piscanec, and A. C. Ferrari, "Edge-functionalized and substitutionally doped graphene nanoribbons: Electronic and spin properties," *Physical Review B: Condensed Matter and Materials Physics*, vol. 77, no. 16, Article ID 165427, 2008.

[11] S. Dutta, A. K. Manna, and S. K. Pati, "Intrinsic half-metallicity in modified graphene nanoribbons," *Physical Review Letters*, vol. 102, no. 9, Article ID 096601, 2009.

[12] Z. Jun, Z. Hui, L. Biao, W. Jianwei, and L. Junwu, "Effects of stone-wales defect symmetry on the electronic structure and transport properties of narrow armchair graphene nanoribbon," *Journal of Physics and Chemistry of Solids*, vol. 77, pp. 8–13, 2015.

[13] N. T. Tien, V. T. Phuc, and R. Ahuja, "Tuning electronic transport properties of zigzag graphene nanoribbons with silicon doping and phosphorus passivation," *AIP Advances*, vol. 8, no. 8, Article ID 085123, 2018.

[14] J. Taylor, H. Guo, and J. Wang, "*Ab initio* modeling of quantum transport properties of molecular electronic device," *Physical Review B: Condensed Matter and Materials Physics*, vol. 63, no. 24, Article ID 245407, 2001.

[15] M. Brandbyge, J.-L. Mozos, P. Ordejon, J. Taylor, and K. Stokbro, "Density-functional method for nonequilibrium electron transport," *Physical Review B: Condensed Matter and Materials Physics*, vol. 65, Article ID 165401, 2002.

[16] J. P. Perdew, K. Burke, and M. Ernzerhof, "Generalized gradient approximation made simple," *Physical Review Letters*, vol. 77, no. 18, pp. 3865–3868, 1996.

[17] H. J. Monkhorst and J. D. Pack, "Special points for Brillouin-zone integrations," *Physical Review B: Condensed Matter and Materials Physics*, vol. 13, no. 12, pp. 5188–5192, 1976.

[18] S. Grimme, "Semiempirical GGA-type density functional constructed with a long-range dispersion correction," *Journal of Computational Chemistry*, vol. 27, no. 15, pp. 1787–1799, 2006.

[19] Z. Nourbakhsh and R. Asgari, "Charge transport in doped zigzag phosphorene nanoribbons," *Physical Review B: Condensed Matter and Materials Physics*, vol. 97, no. 23, Article ID 235406, 2018.

[20] R. Landauer, "Spatial variation of currents and fields due to localized scatterers in metallic conduction," *International Business Machines Journal of Research and Development*, vol. 1, no. 3, pp. 223–231, 1957.

[21] S. Datta, *Electronic Transport in Mesoscopic Systems*, Cambridge University Press, 1997.

[22] G. R. Berdiyorov, H. Bahlouli, and F. M. Peeters, "Effect of substitutional impurities on the electronic transport properties of graphene," *Physica E: Low-dimensional Systems and Nanostructures*, vol. 84, pp. 22–26, 2016.

[23] T. Susi, T. P. Hardcastle, H. Hofsäss et al., "Single-atom spectroscopy of phosphorus dopants implanted into graphene," *2D Materials*, vol. 4, no. 2, Article ID 021013, 2017.

[24] A. Lopez-Bezanilla, W. Zhou, and J. Idrobo, "Electronic and Quantum Transport Properties of Atomically Identified Si Point Defects in Graphene," *The Journal of Physical Chemistry Letters*, vol. 5, no. 10, pp. 1711–1718, 2014.

[25] M. M. Ervasti, Z. Fan, A. Uppstu, A. V. Krasheninnikov, and A. Harju, "Silicon and silicon-nitrogen impurities in graphene: Structure, energetics, and effects on electronic transport," *Physical Review B: Condensed Matter and Materials Physics*, vol. 92, no. 23, Article ID 235412, 2015.

[26] X.-F. Li, K.-Y. Lian, Q. Qiu, and Y. Luo, "Half-filled energy bands induced negative differential resistance in nitrogen-doped graphene," *Nanoscale*, vol. 7, pp. 4156–4162, 2015.

[27] T. Susi, J. Kotakoski, D. Kepaptsoglou et al., "Silicon–carbon bond inversions driven by 60-keV electrons in graphene," *Physical Review Letters*, vol. 113, no. 11, Article ID 115501, 2014.